Quantum Electronics **50** (5) 506–509 (2020)

https://doi.org/10.1070/QEL17238

Distributed fibre-optic temperature sensor for cryogenic applications based on detection of boson components of Raman light scattering

B.G. Gorshkov, G.B. Gorshkov, K.M. Zhukov

Abstract. **The possibility of designing a distributed fibre-optic sensor, allowing one to measure cryogenic temperatures (to liquid nitrogen boiling point), is experimentally demonstrated. The principle of operation of the sensor is based on measuring the intensity of boson peaks of Raman scattering in a fibre material, which are spaced by 1 to 3 THz from the probe frequency. The measurements are performed using a single-mode telecommunication fibre with a 15-μm-thick polyimide coating. The probe wavelength is 1.55 μm, the sensor spatial resolution is 4 m, and the averaging time is 60 s. Experiments are carried out in the temperature range of 75.6 – 79.6 K, with a temperature resolution of 0.5 K.**

Keywords: *distributed sensor, fibre optics, measurements of low temperatures.*

1. Introduction

In recent decades, distributed temperature sensors based on fibre-optic technologies have been actively used in various fields, including oil well monitoring, fire prevention systems, etc. The principle of operation of these sensors is generally based on measuring the Raman scattering intensity in a fibre core material [1] or the Brillouin scattering frequency shift [2, 3]. However, these methods can hardly be used to perform measurements in the temperature ranges corresponding to liquid nitrogen (77 K) or liquefied natural gas (110 K). In particular, the intensity of informative anti-Stokes Raman component at liquid nitrogen temperature decreases almost to zero, and the dependence of Brillouin scattering frequency shift is ambiguous [4]; this ambiguity deteriorates the measurement accuracy.

Let us consider other existing possibilities for measuring cryogenic temperatures. It was shown in [4] that the Brillouin amplification linewidth yields information about the optical fibre temperature. In addition, one can perform low-temperature measurements by measuring the spontaneous Brillouin scattering amplitude [5]. However, being rather complicated, the Brillouin reflectometry can hardly be considered as an adequate solution of the stated problem [6]. In recent years there have been several studies devoted to the principles of measuring temperature changes based on recording elastic (Rayleigh) light scattering reflectograms. In the case of probe frequency scanning, temperature variations are estimated from the shift of Rayleigh scattering spectra [7–9] or from the true phase accumulated due to the temperature effect [10]. A drawback of this method is that one can perform only relative measurements (a reference with respect to which the measurements are performed should be recorded). However, there is another possibility of measuring cryogenic temperatures, which is based on recording boson peak intensity in Raman scattering, as was indicated as early as in 1990 [3]. Later on this issue was developed in [11]; however, neither comprehensive analytical study nor experiments in this field have been performed.

The purpose of this work was to propose (proceeding from experimental data and mathematical simulation) the most appropriate (and simple in realisation) scheme of a distributed low-temperature sensor, based on measuring the intensity of boson Raman peaks, design a breadboard of the corresponding distributed fibre-optic sensor, and estimate its characteristics.

2. Analysis of the measurement method

The experimental spontaneous Raman backscattering spectra for a telecommunication single-mode optical fibre are shown in Figs 1 and 2 (Stokes and anti-Stokes components, respectively). Curves 3 in both figures correspond to a fibre temperature of 300 K. The spectra were recorded using a single-frequency laser diode with a working wavelength of 1551 nm, a circulator, and an Ando AQ 6317 spectrum analyser. Rayleigh scattering was suppressed by a thin-film rejection filter with a bandwidth of 6 nm. The negative sign on the abscissa axis in Fig. 1 indicates a decrease in frequency due to the Stokes Raman shift. These spectra do not differ much from those recorded previously (see, e.g., [3]). It is noteworthy that, along with the well-known bands, spaced by 13 THz from the excitation frequency, there are bands with a smaller frequency shift (1–3 THz), which are generally referred to as boson and have a higher spectral brightness. These spectra are described by the well-known expressions [12]

$$I_{as} = S(\omega)\, n(\omega), \tag{1}$$

$$I_{s} = S(\omega)[1 + n(\omega)], \tag{2}$$

where I_{as} and I_{s} are, respectively, the intensities of anti-Stokes and Stokes Raman components; $S(\omega)$ is the temperature-

B.G. Gorshkov Prokhorov General Physics Institute, Russian Academy of Sciences, ul. Vavilova 38, 119991 Moscow, Russia; e-mail: bggorshkov@gmail.com;
G.B. Gorshkov PetroFibre Ltd, Klinskii pr. 7, 301664 Novomoskovsk, Tula region, Russia;
K.M. Zhukov Laboratory of Electronic and Optical Systems Ltd., Spartakovskaya pl. 14, stroenie 4, 105082 Moscow, Russia

Received 27 December 2019; revision received 11 March 2020
Kvantovaya Elektronika **50** (5) 506–509 (2020)
Translated by Yu.P. Sin'kov

independent function of optical-phonon frequency ω, which describes the band spectral shape;

$$n(\omega) = \{\exp[\hbar\omega/(kT)] - 1\}^{-1} \quad (3)$$

is the Bose function; k is the Boltzmann constant; T is the absolute temperature of the medium; and $\hbar$ is Planck's constant.

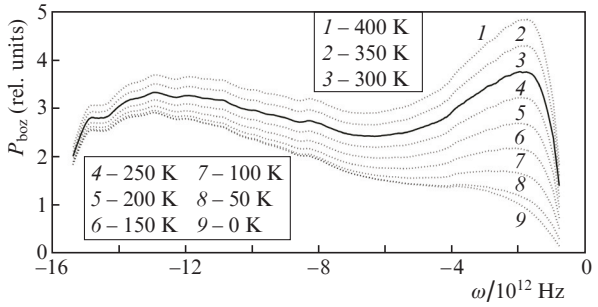

Figure 1. Spectrum of the Stokes Raman component. The shift $\omega = 0$ corresponds to the probe frequency.

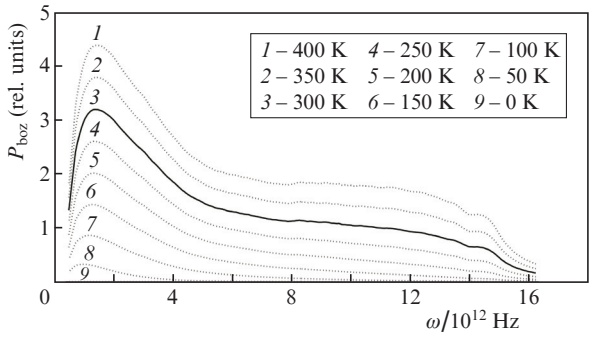

Figure 2. Spectrum of the anti-Stokes Raman component.

Proceeding from formulae (1)–(3) and based on the room-temperature experimental spectra, we calculated the Raman spectra for different fibre temperatures (Figs 1, 2). Their analysis shows that the intensity of the anti-Stokes Raman band spaced from the excitation frequency by 13 THz, which is traditionally used in distributed temperature sensors as the most informative one, is close to zero; hence, the measurement of cryogenic temperatures below 150 K becomes practically impossible. The reason is that the term $n(\omega)$ in (1) and (2) is small at low temperatures, because the efficiency of thermal generation of optical phonons is very low in this case. For the same reason, the Stokes component, even being significant, barely depends on temperature. At the same time, the intensity of the Raman bands spaced by 1–3 THz from the excitation frequency exhibit a close-to-linear temperature dependence, at least, down to 50 K. The measurement of lower temperatures using Raman scattering remains a challenging problem.

Figure 3 shows the dependences of the intensities of boson peaks of anti-Stokes and Stokes Raman components ($\omega = 2$ THz) on absolute temperature. It can be seen that, starting from 50 K, the dependence is close to linear, due to which one can measure temperatures above 50 K with a sufficiently high accuracy. At the same time, the dependence of the anti-Stokes

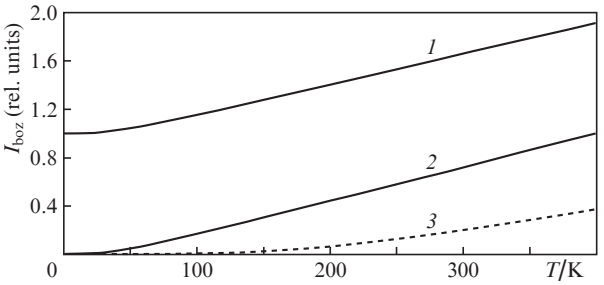

Figure 3. Intensities of the (*1*) Stokes and (*2*) anti-Stokes boson components of Raman scattering, spaced from the probe frequency by 2 THz, and (*3*) anti-Stokes component of Raman scattering, spaced by 13 THz, as functions of absolute temperature.

Raman component ($\omega = 13$ THz) is highly nonlinear at low temperatures, and its intensity is fairly low under these conditions.

3. Experimental

To analyse the possibility of measuring cryogenic temperatures based on boson Raman peaks, we designed an experimental optical time-domain reflectometer (OTDR); its schematic is presented in Fig. 4. A distributed feedback master laser diode (*1*) with a radiation wavelength of 1551 nm at a spectral width of no more than 0.01 nm generates 40-ns pulses. After an erbium amplifier (*2*) the probe radiation is transmitted through a narrowband dense wavelength division multiplexing (DWDM) filter (*3*) with a transmission bandwidth of less than 100 GHz to exclude the contribution of amplifier luminescence to the recorded reflectograms (this radiation is power-modulated with the pulse repetition frequency and may distort the recorded reflectogram). The probe radiation passes through a polarisation scrambler (*4*) (General Photonics PSM-002) and a circulator (*5*) and passes segments of the fibre under test (*6–9*). The probe peak power (1 W) was limited to exclude the occurrence of nonlinear effects, which distort reflectograms. Backscattered radiation passes through the circulator (*5*), a multiplexer (*10*) and filters (*11*) and (*12*) to arrive at photodetectors (*13*) and (*14*) (avalanche photodiodes with a transimpedance amplifier and a bandwidth of 50 MHz). The multiplexer (*10*) allows one to separate the Stokes radiation (13 THz) intensity and the total intensity of boson peaks. Filter *11* with a spectral width is 6 nm (from 1547 to 1553 nm) serves as a rejecter: it cuts off the

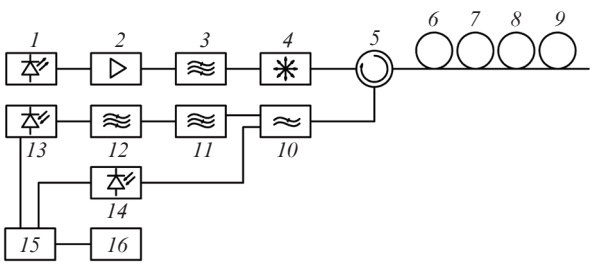

Figure 4. Schematic of the experimental setup: (*1*) master laser diode; (*2*) erbium amplifier; (*3*) narrowband filter; (*4*) polarisation scrambler; (*5*) circulator; (*6–9*) fibres under test; (*10*) spectral multiplexer; (*11*, *12*) filters; (*13*, *14*) photodetectors; (*15*) analog-to-digital converter; (*16*) computer.

Rayleigh scattering signal. Filter *12* (of welded design) with a periodic transmission function suppresses simultaneously the Stokes and anti-Stokes Raman components and transmits their boson components. The spectrum of the boson Raman peaks (we are interested in) at the photodetector input coincides with that reported by us in [13]. The photodetector signal is amplified, digitised by an analog-to-digital converter (*15*) with a frequency of 50 MHz, and stored in the memory of a computer (*16*).

The experiments were performed with optical fibres of two types: an LWP Fujikura fibre with a length of about 8 km, equipped with an epoxy acrylate buffer, and a single-mode fibre with a polyimide coating 155 μm in diameter, which was exposed to low temperatures. It was found that the loss of standard telecommunication fibre at liquid nitrogen temperature exceeds 10 dB km^{-1}, which is unacceptable. We attribute this damping to the microbends arising as a result of the silica fibre deformation by the buffer shell 250 μm in diameter. The use of a fibre with a thin (15 μm) coating solves this problem to a large extent. A fibre portion with a polyimide coating, divided into three successive segments, was welded to a 8-km-long coil (*6*). Segment *8* with a length of 18 m, formed as a free bay 60 mm in diameter, was placed in foamed plastic vessel filled with liquid nitrogen. Segments *7* and *9*, also 18 m long, were maintained at normal temperature. Since we were interested in the temperature resolution of the setup, all experiments were performed directly in the medium of evaporating liquid nitrogen, due to which the temperature was maintained uniformly over the length of fibre bay *8*. To obtain well-controlled temperature variations, the aforementioned vessel with the fibre was placed in a hermetic vessel with a possibility of changing pressure, which was monitored by a pressure-and-vacuum gauge with an accuracy class of 1.5%. Using a vacuum pump and a needle-like valve, we could perform measurements in the pressure range from −0.25 to +0.3 bar, which corresponds to a change in temperature from 75.6 to 79.5 K [14].

The measurements showed (as was expected) that the intensity of the Stokes Raman component (13 THz) barely depends on temperature; hence, to exclude additional noise, this component was neglected in calculations.

The reflectogram for the sum of boson components at $T = 77$ K is shown in Fig. 5. The spatial resolution is 4 m. The fibre segment with coordinates of 8184–8202 m was at liquid nitrogen temperature, and the other segments were at 300 K.

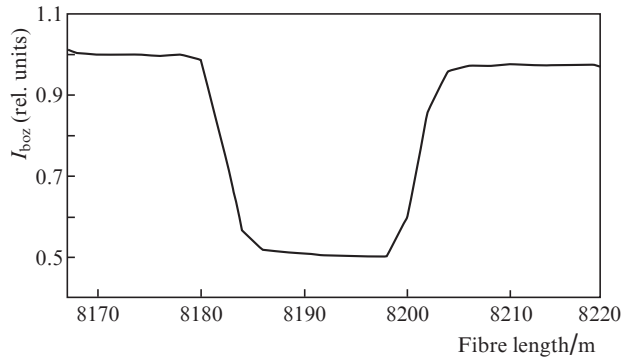

Figure 5. Reflectogram for the sum of boson components (bay *8* at a temperature of 77.4 K).

The temperature dependence of the boson component intensity I_{boz} and its linear approximation are shown in Fig. 6. It can be seen that the intensity I_{boz} changes linearly with temperature, in correspondence with the temperature dependence of saturated nitrogen vapour pressure [14] (in the temperature range of 75–80 K this dependence can be considered as linear).

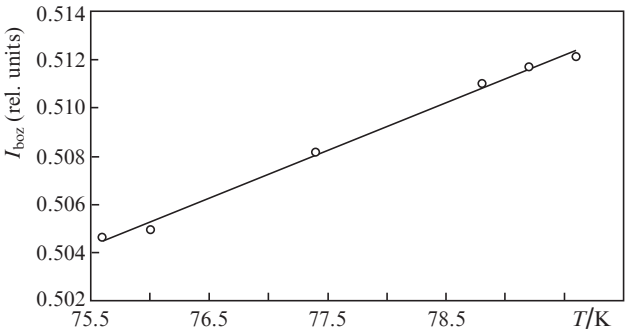

Figure 6. Temperature dependence of the boson component intensity and its linear approximation.

The temporal run of measured I_{boz} values is shown in Fig. 7. The horizontal segments with indicated temperature denote the time intervals during which this temperature was maintained.

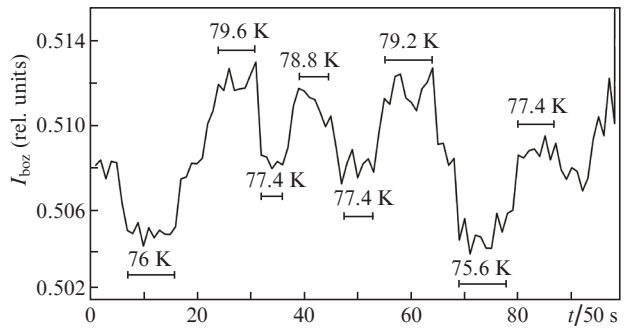

Figure 7. Temporal run of the experiment.

Note that the characteristics obtained by us are not limiting. In particular, at the aforementioned spatial resolution, the photodetection modules in use have a nonoptimal (excessively wide) reception bandwidth; the spectral characteristics of optical filters are neither optimal. The low-temperature sensitivity can be somewhat improved by detecting only the anti-Stokes part of the boson component. The probe pulse frequency can be increased for shorter distances, due to which the signal-to-noise ratio can be improved. At the same time, the question about the optimal design of the optical fibre providing low loss at cryogenic temperatures remains open.

Thus, the possibility of designing a distributed fibre-optic sensor for measuring cryogenic (77 K) temperatures was experimentally shown for the first time based on measuring the intensity of boson peaks in Raman scattering spectra. A sensitivity at a level of 0.5 K at a spatial resolution of 4 m and a signal acquisition time of 50 s was demonstrated.

Acknowledgements. We are grateful to M.A. Taranov for his interest in the study and valuable remarks.

References

1. Dakin J.P. Patent UK, GB2140554A (1984).
2. Gorbatov I.E., Gorshkov B.G. *Fiz. Tverd. Tela*, **30**, 2226 (1988).
3. Gorshkov B.G., Gorbatov I.E., Danileiko Yu.K., Sidorin A.V. *Sov. J. Quantum Electron*., **20**, 283 (1990) [*Kvantovaya Elektron*., **17**, 345 (1990)].
4. Thévenaz L., Alexandre Fellay A., Facchini M., Scandale W., Niklès M., Robert P.A. *Proc. SPIE*, **4694**, 22 (2002).
5. Mahar S., Geng J., Schultz J., Minervini J., Jiang S., Titus P., Takayasu M., Gung C., Tian W., Chavez-Pirson A. *Proc. SPIE*, **7087**, 70870I-1 (2008).
6. Hartog A.H. *An Introduction to Distributed Optical Fibre Sensors* (Taylor & Francis Group, LLC, 2017).
7. Koyamada Y., Imahama M., Kubota K., Hogari K. *J. Lightwave Technol.*, **27**, 1142 (2009).
8. Lu X., Soto M.A., Thévenaz L. *Proc. SPIE*, **9157**, 91573R (2014).
9. Gorshkov B.G., Taranov M.A., Alekseev A.E. *Laser Phys.*, **27**, 085105 (2017).
10. Nikitin S.P., Kuzmenkov A.I., Gorbulenko V.V., Nanii O.E., Treshchikov V.N. *Laser Phys.*, **28**, 085107 (2018).
11. Rabia M.K., Jurdyc A.M., Le Brusq J., Champagnon B., Vouagner D. *Opt. Laser Technol.*, **94**, 25 (2017).
12. Cardona M. (Ed.) *Light Scattering in Solids* (Heidelberg: Springer, 1975).
13. Gorshkov B.G., Gorshkov G.B., Zhukov K.M. *Quantum Electron*., **49**, 581 (2019) [*Kvantovaya Elektron*., **49**, 581 (2019)].
14. *Razdelenie vozdukha metodom glubokogo okhlazhdeniya. Tekhnologiya i oborudovanie* (Air Separation by Deep Cooling. Engineering and Equipment) (Moscow: Mashinostroenie, 1973) Vol. 1, p. 91.